

Discovery of a redshifted Iron K–line in the X–ray afterglow of GRB 000214.

L.A. Antonelli¹, L. Piro², M. Vietri³, E. Costa², P. Soffitta², M. Feroci², L. Amati⁴, F. Frontera^{4,5}, E. Pian⁴, J.J.M. in 't Zand⁶, J. Heise⁶, E. Kuulkers⁶, L. Nicastro⁷, R.C. Butler^{4,8}, L. Stella^{1,9}, and G.C. Perola³

Received _____; accepted _____

¹Osservatorio Astronomico di Roma, Via Frascati, 33, 00040, Monteporzio Catone (Roma), Italy.

²Istituto di Astrofisica Spaziale, C.N.R., Area della Ricerca di Tor Vergata, Via Fosso del Cavaliere, 100, 00133, Roma, Italy.

³Università degli Studi “Roma Tre”, Via della Vasca Navale, 84, 00146, Roma, Italy.

⁴Istituto Tecnologie e Studio delle Radiazioni Extraterrestri, C.N.R., Via Gobetti, 101, 40129, Bologna, Italy.

⁵Dipartimento di Fisica, Università di Ferrara, Via del Paradiso, 12, 52100, Ferrara, Italy.

⁶Space Research Organization Netherlands, Sorbonnelaan, 2, 3584 CA Utrecht, Netherlands.

⁷Istituto di Fisica Cosmica e Applicazioni Calcolo Informatico, C.N.R., Via La Malfa, 153, 90138, Palermo, Italy.

⁸Agenzia Spaziale Italiana, Viale della Regina, 212, 00100, Roma, Italy.

⁹Affiliated to the International Center for Relativistic Astrophysics

ABSTRACT

We report the detection (3σ significance level) of a strong iron emission line in the X-ray spectrum of the afterglow of GRB 000214 (“Valentine’s Day Burst”) observed by BeppoSAX. An emission line feature was observed with a centroid energy of 4.7 ± 0.2 keV which, if interpreted as $K\alpha$ emission from hydrogen-like iron, corresponds to a redshift of $z=0.47$. The intensity ($EW \sim 2$ keV) and duration (tens of hours) of the line give information on the distance, from the burst region, of the emitting material ($R \geq 3 \times 10^{15}$ cm) and its mass ($M \geq 1.4M_{\odot}$). These results are not easily reconciled with the binary merger and hypernova models for gamma ray bursts, because they require large amounts of mass (about $1M_{\odot}$), at large distances ($\approx 10^{16}$ cm), and at newtonian speeds.

Subject headings: gamma rays: bursts—line: formation—X-rays: general

1. Introduction

Three years after the first identification of the X-ray afterglow from a Gamma Ray Burst (GRB) (Costa et al., 1997), the nature of Gamma Ray Bursts’ progenitors remains uncertain. The most widely discussed theoretical models for GRBs consider vastly different scenarios both in terms of the progenitors and environment. If the GRBs originate from neutron star-neutron star or neutron star-black hole mergers (Narayan, Paczynski and Piran 1992) then, for about a half of all GRBs, the explosion should be located far from the place where the progenitor binary system was formed and most probably in a low-density interstellar medium. On the other hand, if GRBs originate from Hypernovae (Paczynski, 1998; Woosley, 1993) or SupraNovae (Vietri & Stella, 1998), the immediate progenitor is a massive, rotating star, and thus the explosion should take place in a high density medium,

probably a star-forming region. The discovery of emission lines in the X-ray spectrum of a GRB afterglow represents a major step toward the understanding of the nature of GRB progenitors. In fact, the measurement of X-ray lines emitted by a GRB or its afterglow provides a direct measurement of the redshift and a powerful diagnostic of both the nature of the central engine and the environment in which GRBs go off (Perna & Loeb, 1998; Mészáros & Rees, 1998; Böttcher et al., 1999, Ghisellini et al., 1999; Paerels et al., 2000). Other methods, such as collecting offsets between GRBs afterglow and their host galaxies (Bloom et al., 1999) or searching for absorbing material between the GRB and the observer (Wijers & Galama, 1999; Owens et al., 1999), are comparatively less direct.

Presently, there are only two marginal detections of an X-ray emission line in GRB afterglows, one in GRB 970508 (chance probability for a statistical fluctuation of 0.7%, Piro et al. 1999) and one in GRB 970828 (probability of 1.7%, Yoshida et al. 1999). The presence of a strong iron line in the X-ray spectrum of a GRB afterglow implies a rich environment located very close to the GRB region and may be an important clue in favor of collapsar models (Mészáros & Rees, 1998; Lazzati, Campana, & Ghisellini, 1999; Weth et al., 2000; Vietri et al., 1999). In fact, in the case of the Hypernova scenario an iron rich circumburst environment may be produced by the stellar wind before the explosion of the Hypernova (Mészáros & Rees, 1998). A similarly favorable situation occurs in the SupraNova scenario (Vietri & Stella, 1998) where a supernova explosion precedes by a few months the GRB event. GRB 000214 (“Valentine’s Day Burst”) has no optical nor near-infrared afterglow (Rhoads et al., 2000; Wijers et al., in preparation) as is the case for about half of all GRBs with follow-up observations (e.g., Kulkarni et al., 2000). The lack of optical and IR counterparts to a GRB may result from extinction in a dense surrounding medium; therefore, searching for emission lines in the X-ray afterglows of these GRBs looks especially promising. Based on a BeppoSAX pointed observation of GRB 000214, we report on the detection of an Iron $K\alpha$ line from its X-ray afterglow.

2. Observation and results

GRB 000214 was detected both by the Gamma Ray Burst Monitor (GRBM) and Wide Field Cameras (WFC) on-board BeppoSAX on 2000 Feb. 14 01:01:01 UT. The prompt event, i.e. the gamma ray emission detected by GRBM, lasted ~ 10 s and had a fluence of $\mathcal{F}=1.4 \times 10^{-5}$ erg cm $^{-2}$ in the 40–700 keV band. The corresponding prompt X-ray emission detected by WFC had a fluence of $\mathcal{F}=1.0 \times 10^{-6}$ erg cm $^{-2}$ (2–10 keV). In the X-rays a complex multi-peaked structure lasting about 2 min after the burst proper was clearly seen; a detailed analysis of the early behaviour of GRB 000214 will be presented elsewhere. The evolution of the X to Gamma-ray spectrum from the prompt event showed a spectral softening similar to that observed in other GRBs (Frontera et al., 1998, 2000a, 2000b).

2.1. Narrow Field Instruments observation

A follow-up observation with the BeppoSAX Narrow Field Instruments (NFI) began about 12 hours after the burst and lasted about 104,000 s. The effective exposure time was 51,000 s on source time for the BeppoSAX Medium Energy Concentrator/Spectrometer (MECS), and 15,000 s in the Low Energy Concentrator/Spectrometer (LECS). A previously unknown X-ray source, 1SAX J1854.4-6627, was detected in the MECS and LECS field of view at a position of RA = $18^h 54^m 27^s.0$ and DEC = $-66^\circ 27' 30''$ (J2000) (uncertainty radius of 50"). The source position lies within the WFC error circle (Paolino et al., 2000; Antonelli, 2000) and IPN error box (Hurley & Feroci, 2000). The 2–10 keV flux of 1SAX J1854.4-6627 decreased by a factor of about two, from $(7.7 \pm 0.8) \times 10^{-13}$ (first 11 ks) to $(4.2 \pm 0.7) \times 10^{-13}$ erg cm $^{-2}$ s $^{-1}$ (last 10 ks), during the BeppoSAX observation (these fluxes were derived by using the best fit model to the spectra, see next section). In consideration of its fading behaviour and position within both the WFC and IPN error boxes, we concluded that 1SAX J1854.4-6627 represents the afterglow of GRB 000214.

The MECS lightcurve yields a flux decay ($F(t) \propto t^{-\beta}$) with $\beta = (0.8 \pm 0.5)$ (hereafter all errors are quoted at 90% confidence level for one parameter of interest). Combining the MECS lightcurve with the WFC lightcurve from after the main event (extending for 39 s after burst onset) yields a flux decay with a power-law slope of $\beta = (1.41 \pm 0.03)$. This slope is somewhat steeper than usually observed in GRB X-ray afterglows ($\beta \simeq 1.2$).

2.2. Spectral analysis of GRB 000214 X-ray afterglow

We extracted the LECS(0.1-4.0 keV) and MECS(1.6-10.0 keV) spectra of the source from the entire BeppoSAX observation (figure 1) using standard procedures (Fiore et al., 1999)¹⁰. The extraction regions were chosen so as to maximize the signal-to-noise ratio. An accurate analysis of local background was performed in order to check for spurious features. After having verified that the local background is compatible with that derived from blank field observations available at the BeppoSAX Science Data Center, we used the latter in order to achieve a background subtraction with improved signal to noise (see also figure 2). Both the LECS and MECS spectra were binned so as to have at least 15 photons per bin. Spectral analysis was performed using the XSPEC10.0 package. We checked that our results are nearly insensitive to the details of the background subtraction.

We first fit the data with a power-law plus photoelectric absorption. The relative normalization of LECS versus MECS was left free to vary in the 0.7-1.0 range (Fiore et al., 1999). We obtained a best-fit value of $\chi^2 = 25.4$ for 14 (d.o.f.). The column density best-fit value ($N_H = 0.7^{+7.5}_{-0.7} \times 10^{20} \text{ cm}^{-2}$) is compatible with the Galactic value $N_H = 5.5 \times 10^{20} \text{ cm}^{-2}$ (Dickey & Lockman, 1990), so we fixed it to this value. We obtained a power-law

¹⁰Fiore, F., Guainazzi, M., & Grandi, P., 1999, Cookbook for BeppoSAX NFI Spectral Analysis, (<http://www.sdc.asi.it/software/>)

photon index of $\Gamma = 2.0 \pm 0.3$ and a flux of $F_x(2 - 10 \text{ keV}) = (2.75 \pm 0.9) \times 10^{-13} \text{ erg cm}^{-2} \text{ s}^{-1}$. The best-fit value was $\chi^2 = 27.5$ for 15 (d.o.f.). These relatively high chisquare values (corresponding to a chance probability of $P_\chi(\chi^2, \nu) \simeq 0.02$ in the latter case) justified a deeper analysis. The residuals to the fit above show a clear excess around energies of $\sim 4 - 5 \text{ keV}$ which can be interpreted as an emission line (see figure 1). We added a narrow (with respect to MECS energy resolution, which is $\Delta E/E = 8 \times (E/6 \text{ keV})^{-0.5} \text{ FWHM}\%$) Gaussian line to the previous model in order to fit the observed feature. We inferred in this way a line centroid energy of $E = 4.7 \pm 0.2 \text{ keV}$ and an intensity of $I_l = (9 \pm 3) \times 10^{-6} \text{ photons cm}^{-2} \text{ s}^{-1}$, translating into an E.W. of $\sim 2.1 \text{ keV}$. The best fit chisquare value was $\chi^2 = 11.5$ for 13 d.o.f. Applying an F -test to assess the statistical significance of the Gaussian feature we obtained a chance probability of 0.27% (corresponding to 3.0σ significance level). The other spectral parameters were only marginally affected by the inclusion of the Gaussian, with a power-law photon index of $\Gamma = 2.2 \pm 0.3$ and a flux of $F_x(2 - 10 \text{ keV}) = (2.9 \pm 0.9) \times 10^{-13} \text{ erg cm}^{-2} \text{ s}^{-1}$. The LECS normalization relative to the MECS depends mainly on the source position in the LECS and the different exposure intervals than the MECS (note that the source was fading). However the statistical uncertainty we determined for this normalization was greater than the nominal range; therefore we also fixed it to 0.8, the value inferred from a BeppoSAX observation of NGC 7469 (Piro et al.1999b), a Seyfert 1 galaxy with a $0.1 - 10 \text{ keV}$ spectrum similar to that of the GRB 000214 afterglow. The best fit chisquare value was $\chi^2 = 28$ for 16 d.o.f. fitting data with the simple power-law model and $\chi^2 = 12.1$ for 14 d.o.f. adding a Gaussian line to the previous model. Following this procedure, while the spectral parameters remain essentially unchanged a slightly improved statistical significance (F -test) was obtained for the fit with the power-law and Gaussian line (chance probability of 0.15%, or $\sim 3.2\sigma$).

We divided the MECS observation in two consecutive intervals (20 ks and 30 ks exposure). MECS spectra were extracted from each interval by the same method as

above. As shown in figure 3 both spectra show evidence for an emission line at an energy compatible, within the errors, with the line detected during the entire observation. Note also that most of the flux decrease in the second part of the observation seems due to the continuum rather than the line. Poor statistics does not allow a more quantitative investigation.

3. Discussion and conclusions

The only cosmologically abundant element that can produce lines beyond 4 keV is iron, provided one precludes Doppler shifts to shorter wavelengths. Iron emits a $K\alpha$ line photons with an energy between 6.4 (for the lower ionization stages of iron) and 6.95 keV (for hydrogen-like iron). The observed feature may be also interpreted as the Iron recombination K-edge at 9.28 keV (corresponding to a redshift of $z = 0.9$) but, in such a case, according to Weth et al. (2000), we should expect both a Fe K-edge and a $K\alpha$ line having about the same intensity. The Fe- $K\alpha$ line should be redshifted at an energy between 3.2 and 3.5 keV but no line is detected in the MECS spectrum of GRB 000214 afterglow within this range. If we identify the emission feature in GRB 000214 as Fe $K\alpha$, the corresponding redshift is between $z = 0.37$ and 0.47 . We will assume $z = 0.47$ for simplicity, but none of the following discussion hinges upon this exact value.

The case of GRB 000214 differs from that of GRB 970508 in two ways. First, the iron line is more significant in GRB 000214: we find that the probability of a chance fluctuation is 0.27%, as compared to 0.7%. This difference becomes even more remarkable when one considers that there is no independent determination of the redshift for GRB 000214, while GRB 970508 has $z = 0.835$ from optical observations (Metzger et al., 1997). Second, the afterglow observation of GRB 000214 did not allow detection of a possible reburst, contrary to GRB 970508. In fact, GRB 000214 was observed just once after the burst proper,

beginning 12 h after the main event, and for a total of $\approx 10^5$ s. GRB 970508, instead, was observed on four different occasions after the burst, beginning 6 h after the main event, with the last set of observations more than 6 days after the burst (Piro et al., 1999). Thus, for GRB 000214, we have no time coverage to exclude a reburst before or after the time of our observations: all we can say is that, during this limited time, the flux decreased by about a factor of 2 (see Section 2.1). This is consistent with GRB 970508, where the line was bright as the flux was decreasing (Fig. 2a of Piro et al., 1999); thus the model of Vietri et al. (1999), connecting the appearance of the iron line to the reburst, is still viable.

For $z = 0.47$, $H_o = 70 \text{ km s}^{-1} \text{ Mpc}^{-1}$, and $\Omega = 1$, we find a total energy release, in the line only, of $E_l = 3 \times 10^{48} \text{ erg}$, i.e. $N_l = 3 \times 10^{56}$ photons emitted within the first $t_d \approx 10^5$ s after the burst; the emission is isotropic because the line is sub-relativistic. If each iron atom were to emit a single line photon, then $M_{Fe} \approx 12M_\odot$, way too large. Thus each iron atom must produce several line photons (Lazzati et al., 1999), and, consequently, the time-scale t_{Fe} over which every iron atom produces a photon satisfies $t_{Fe} \ll t_d \approx 10^5$ s, and does not seem to begin fading. This implies that the time-scale t_d is set by the geometrical factor: the line-emitting material must be located at $R \gtrsim 3 \times 10^{15} \text{ cm}$, and we are seeing some sizeable fraction of it.

The minimum iron mass is determined by Lazzati et al.(1999) as

$$M_{Fe} \geq 5 \times 10^{-3} M_\odot \frac{F_{-13} t_5 R_{16}^2}{q E_{50}} \quad (1)$$

where $F_{-13} \approx 0.5$ is the line luminosity in units of $10^{-13} \text{ erg cm}^{-2} \text{ s}^{-1}$, $t_5 \approx 1$ is the line duration in units of 10^5 s , $R_{16} \approx 0.3$ the material distance in units of 10^{16} cm , q is the fraction of the absorbed ionizing fluence and reprocessed into the line ($q \lesssim 0.1$ as derived by Ghisellini et al., 1999) and E_{50} is the total X-ray burst luminosity in units of 10^{50} erg ; for GRB 000214 we find $E_{50} \approx 8$ if the burst emission were isotropic. With these values

$$M_{Fe} \gtrsim 2.4 \times 10^{-3} M_\odot . \quad (2)$$

This argues against a possible origin of this GRB in a neutron star - neutron star (or neutron star - black hole) binary merger. The problem is not one of total iron content of the model: for realistic parameters, this scenario can easily satisfy the above limit. The problem lies instead in the capacity of the model to deposit this much iron at these large distances, and at Newtonian speeds. In fact, under our assumption that the line is not blueshifted (at least, its Lorentz factor is ≈ 1), the iron cannot have been released in the burst event itself: there is not time enough for matter ejected in the explosion to rush ahead of photons, slow down, and then be hit by the burst flash. The material generating the line must have been released well before the burst. Given their lack of atmospheres and winds, the only mechanism capable of releasing matter from inspiralling neutron stars is tidal interaction. A mass loss estimate for this process by Mészáros and Rees (1992) has a lower limit of $M_{th} = 4 \times 10^{30} g$, enough to account (barely!) for Eq. 2, but this optimistically assumes that the typical viscosity damping time-scale equals the light travel time across the star (Bildsten and Cutler 1992). Though the exact amount of viscosity in a neutron star is not well-known, theoretical arguments fall short of the amount required for the correctness of the estimate by Mészáros and Rees (1992), by about a factor 2000 (Kochanek 1992, Eq. 4.7, Bildsten and Cutler 1992, see the discussions after Eq. 9 and 16).

In hypernova models, an intense wind should characterize the massive progenitor before the collapse. Calling A the iron mass fraction relative to the solar abundance (Lang 1991, p. 84), we expect from Eq. 2 a minimum mass of

$$M \geq 1.4M_{\odot} \frac{1}{AE_{50}} . \quad (3)$$

The radial mass distribution from a massive stellar wind is $dM = \dot{M}dr/v_{\infty}$. The most extreme ratios of stellar wind mass loss rate \dot{M} to asymptotic speed v_{∞} occur in Luminous Blue Variables and Red SuperGiant Variables ($\dot{M} = 10^{-4}M_{\odot} \text{ yr}^{-1}$, $v_{\infty} = 10 - 100 \text{ km s}^{-1}$, Lamers, 1995, van Loon et al., 1999). For these winds, at $R \approx 3 \times 10^{15} \text{ cm}$ there can

only be $M \approx 10^{-2} - 10^{-3} M_{\odot}$, missing the above lower limit by 2 – 3 orders of magnitude. The densest circumstellar envelopes around the progenitors of some peculiar core collapse supernovae (*e.g.* $n \sim 10^8 - 10^9 \text{ cm}^{-3}$ at $R \sim 3 \times 10^{15} \text{ cm}$ in SN1997ab, Salamanca et al., 1998) imply a mass of $M \sim 10^{-1} - 10^{-2} M_{\odot}$, substantially lower than required by Eq. 3. A model immune from these inconsistencies is the SupraNova, where a core collapse supernova explosion precedes the GRB event by months to years (Vietri and Stella 1998).

On the other hand, the lack of large amounts of material along the line of sight, as testified by the absence of photoelectric soft X-ray absorption on top of the Galactic value¹¹, and the development of a normal X-ray afterglow, clearly suggest the presence of outlying material located in the progenitor’s equatorial plane, at large angles from the line of sight. This material may be either left over from the progenitor’s formation process (as in a primordial gas cloud) or spewed out by the progenitor. Key future observations capable of discriminating between these possibilities will be the measurement of the line width, and a search of atomic species produced in the interiors of evolved stars. Velocities of $\gtrsim 1000 \text{ km s}^{-1}$ can rule out any primordial cloud and/or hypernovae winds; the detection of cobalt or nickel may establish the recent origin of the material from a SN explosion.

This research is supported by the Italian Space Agency (ASI) and Consiglio Nazionale Ricerche of Italy. Beppo-SAX is a joint program of ASI and the Netherlands Agency for Aerospace Programs (NIVR). We thank all members of the Beppo-SAX SDC, SOC and OCC. We also thank L. Burderi, G.L. Israel, F. Fiore, G.Matt and G. Bono and an anonymous referee for helpful comments.

¹¹The upper limit derived above, $N_H = 2.7 \times 10^{20} \text{ cm}^{-2}$, for the non-Galactic column density, corresponds to a total mass, within 12 light hours, of $5 \times 10^{-6} M_{\odot}$, which could indicate a large amount of mass only for implausibly large ($\approx 1 - 10^{-6}$) ionization fractions.

REFERENCES

- Antonelli, L.A., et al., 2000, GCN Circ. #561
- Antonelli, L.A., 2000, GCN Circ. #559
- Bildsten L., Cutler, C., 1992, ApJ, 400, 175.
- Bloom et al., 1999, ApJL, 518, 1
- Böttcher, M., Dermer, C.D.D., Crider, A.W., & Liang, E.D., 1999, A&A, 343, 111
- Costa et al., 1997, Nature, 387, 783
- Dickey & Lockman, 1990, ARAA, 28, 215
- Frontera F. et al., 1998, ApJ, 493, 67
- Frontera F. et al., 2000a, ApJ, in press
- Frontera, F. et al., 2000b, ApJS, 127, 59
- Ghisellini, G., Haardt, F., Campana, S., Lazzati, D., & Covino, S., 1999, ApJ, 517, 168
- Hurley, K. & Feroci, M., 2000, GCN Circ. #556
- Kulkarni, S.R., et al., 2000, preprint (astro-ph/0002168)
- Lamers, H.J.G.L.M., 1995, in IAU Colloq. 155, Astrophysical applications of stellar pulsation, eds. Stobie R.S. & Whitelock P.A., (San Francisco: ASP), 176
- Lang, K.R., 1991, Astrophysical Data: planets and stars, Berlin, Springer & Verlag, 84
- Lazzati, D., Campana, S., & Ghisellini, G., 1999, MNRAS, 304, L31
- Mészáros & Rees, 1998, MNRAS, 299, L10
- Mészáros & Rees, 1992, ApJ, 397, 570.
- Metzger, M.R., et al., 1997, Nature, 387, 378.
- Narayan, R., Paczynski, B., Piran, T., 1992, ApJ, 395, L83

- Owens, A., et al., 1998, *A&A*, 339, 370
- Paczynski, B., 1998, *ApJ*, 494, L95
- Paerels, F., Kuulkers, E., Heise, J., Liedahl, D.A., 2000, *ApJ*, 535, L25
- Paolino, A., et al., 2000, *GCN Circ.* #557
- Perna, R., & Loeb, A., 1998, *ApJ*, 503, L135
- Piro et al., 1999, *ApJ*, 514, L73
- Piro, L., et al., 1999b, *Astron. Nach.*, in press
- Rhoads, J., Wilson, A., Storchi-Bergmann, T., & Fruchter, A., 2000, *GCN Circ.* #564
- Salamanca, I., Cid-Fernandes, R., Tenorio-Tagle, G., Telles, E., Terlevich, R.J., Munoz-Tunon, C., 1998, *MNRAS*, 300, L17
- van Loon, J.Th., et al., 1999, *A&A*, 351, 559
- Vietri, M., Perola, G.C., Piro, L., Stella, L., 1999, *MNRAS*, 308, L29.
- Vietri M. & Stella L., 1998, *ApJ*, 507, L45
- Yoshida, A., et al, 1999, *A&AS*, 138, 433
- Weth, C., Mészáros, P., Kallman, T., Rees, M. J., 2000, *ApJ*, 534, 581
- Wijers, R. & Galama, T., 1999, *ApJ*, 523, 177
- Wijers, R., et al., 2000, in prep.
- Woosley, S.E., 1993, *ApJ*, 405, 273.

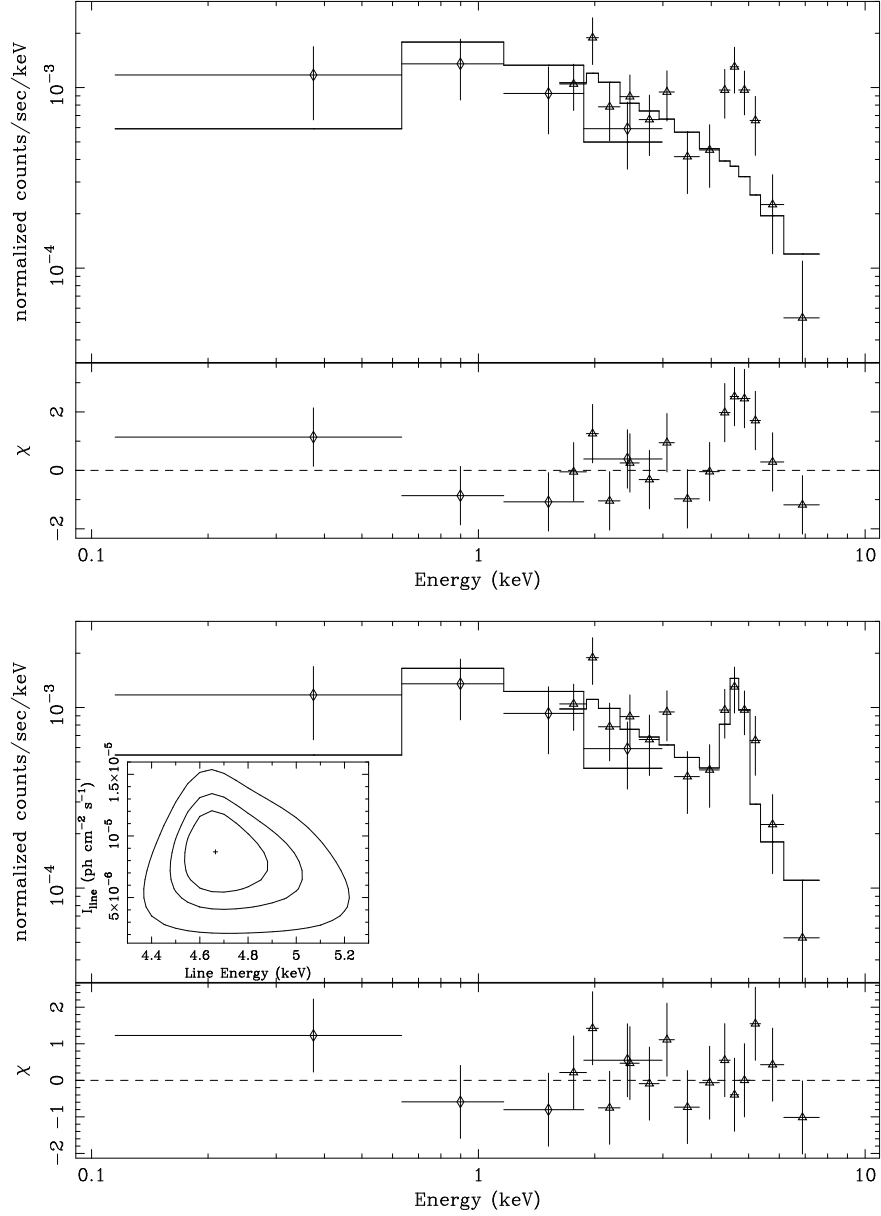


Fig. 1.— BeppoSAX (0.1–10.0 keV) spectra of GRB 000214 X-ray afterglow. LECS points (0.1–3.0 keV): open diamonds, MECS points (1.6 – 10.0 keV): open triangles. *Top panel:* LECS+MECS spectra fitted with an absorbed power-law; an excess around 4.7 keV is clearly seen in the residuals. *Bottom panel:* LECS+MECS spectra fitted with an absorbed power-law plus a narrow Gaussian line. The inset shows the contour plot of the line intensity vs energy. Contours correspond to 68%, 90% and 99% confidence levels for two interesting parameters.

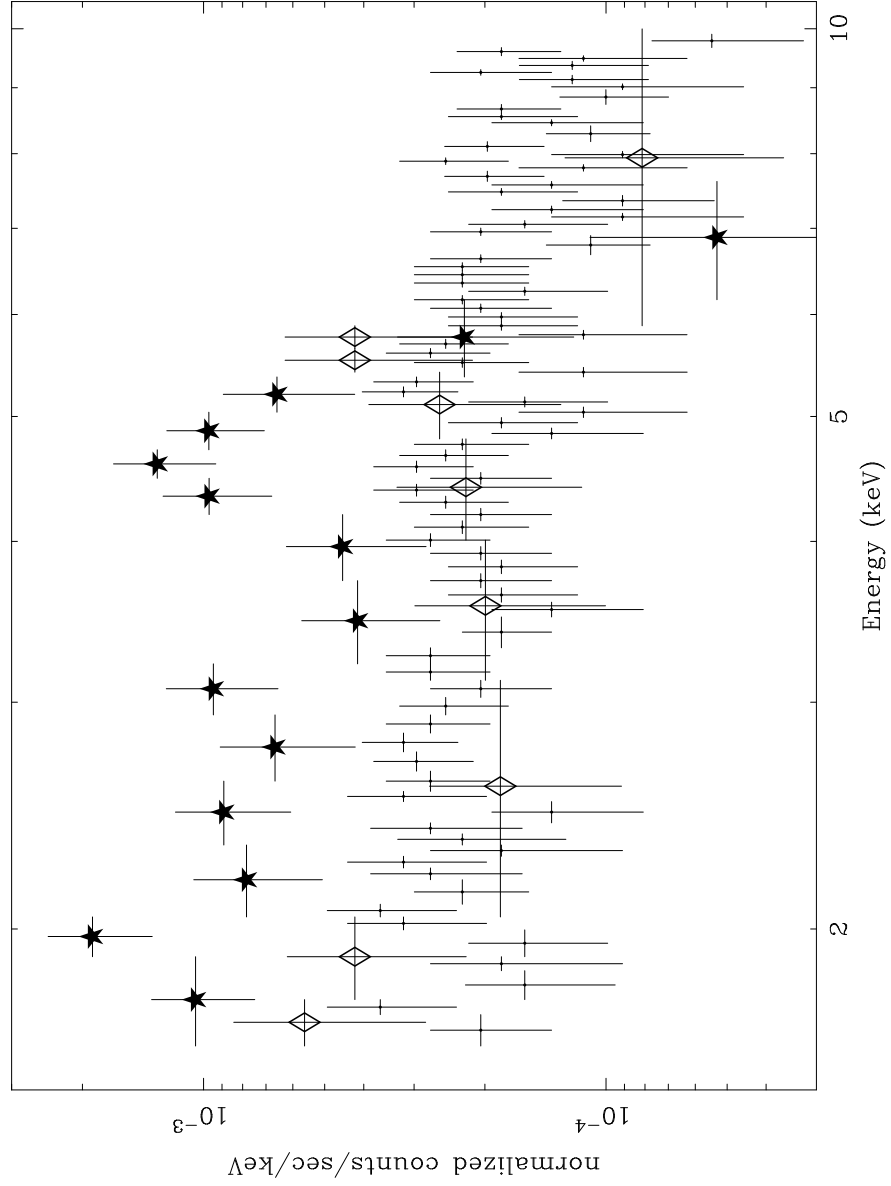


Fig. 2.— Background-subtracted MECS spectrum of GRB 000214 X-ray afterglow (filled stars) compared to the local background (open diamonds) and library background (dots) spectra. The feature centered around 4-5 keV is about a factor of five higher than the background.

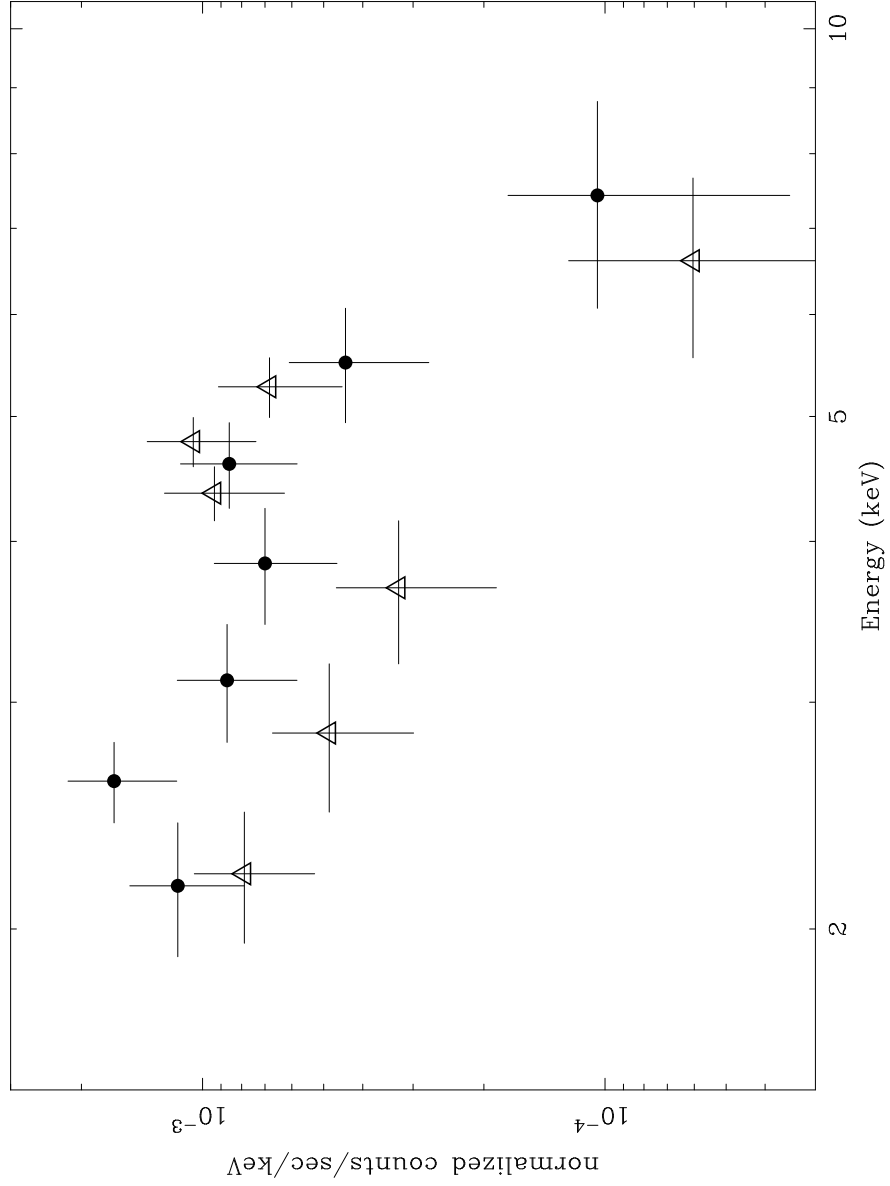


Fig. 3.— 2–10 keV MECS spectrum from the first 20 ks of the observation (filled dots) compared to the spectrum from the last 30 ks (open triangles). Despite poor statistics, there is indication that in the second part of the observation the continuum faded by a factor of about two, while the excess around 4–5 keV remained constant.